

Kosterlitz-Thouless transition and vortex-antivortex lattice melting in two-dimensional Fermi gases with p - or d -wave pairing

Gaoqing Cao,^{1,2} Lianyi He,³ and Xu-Guang Huang^{2,4}¹*School of Physics and Astronomy, Sun Yat-Sen University, Guangzhou 510275, China*²*Department of Physics and Center for Particle Physics and Field Theory, Fudan University, Shanghai 200433, China*³*State Key Laboratory of Low-Dimensional Quantum Physics and Department of Physics, Tsinghua University, Beijing 100084, China*⁴*Key Laboratory of Nuclear Physics and Ion-beam Application (MOE), Fudan University, Shanghai, China 200433*

(Received 28 July 2017; revised manuscript received 20 November 2017; published 22 December 2017)

We present a theoretical study of the finite-temperature Kosterlitz-Thouless (KT) and vortex-antivortex lattice (VAL) melting transitions in two-dimensional Fermi gases with p - or d -wave pairing. For both pairings, when the interaction is tuned from weak to strong attractions, we observe a quantum phase transition from the Bardeen-Cooper-Schrieffer (BCS) superfluidity to the Bose-Einstein condensation (BEC) of difermions. The KT and VAL transition temperatures increase during this BCS-BEC transition and approach constant values in the deep BEC region. The BCS-BEC transition is characterized by the nonanalyticities of the chemical potential, the superfluid order parameter, and the sound velocities as functions of the interaction strength at both zero and finite temperatures; however, the temperature effect tends to weaken the nonanalyticities compared to the zero-temperature case. The effect of mismatched Fermi surfaces on the d -wave pairing is also studied.

DOI: [10.1103/PhysRevA.96.063618](https://doi.org/10.1103/PhysRevA.96.063618)

I. INTRODUCTION

It was proposed by Eagles [1] and Leggett [2] several decades ago that in a many-fermion system with attractive interaction, one can realize an evolution from the Bardeen-Cooper-Schrieffer (BCS) superfluidity to Bose-Einstein condensation (BEC) of difermion molecules by gradually increasing the strength of the interaction. For s -wave interaction, such a BCS-BEC evolution is a smooth crossover [3–11], which has been experimentally studied by using the dilute ultracold fermionic atoms [12–14], where the interaction strength is tuned by means of the Feshbach resonance. Such a dilute ultracold-atomic system is characterized by a dimensionless parameter $1/(k_F a_s)$, where a_s is the s -wave scattering length of the short-range interaction and k_F is the Fermi momentum in the absence of interaction. The BCS-BEC crossover occurs when $1/(k_F a_s)$ goes from $-\infty$ to ∞ . In addition, the Anderson-Bogoliubov collective mode of fermionic superfluidity at weak attraction evolves smoothly to the Bogoliubov excitation of weakly repulsive Bose condensate at strong attraction [5,11,15–17].

On the other hand, for nonzero orbital-angular-momentum pairing, such as p - or d -wave pairing, the BCS-BEC evolution is not smooth but associated with some quantum phase transition [18–25]. Such a quantum phase transition cannot be characterized by a change of symmetry or the associated order parameter. Instead, different quantum phases can be distinguished topologically [18]. Recently, the p -wave Feshbach resonance has been realized in three-dimensional ultracold Fermi gases of ^{40}K [26] and bosonic $^{85}\text{Rb} - ^{87}\text{Rb}$ mixture [27], and some of the predicted universal relations for p -wave interaction [28,29] were successfully verified. On the other hand, the two-dimensional (2D) systems are of particular interest since the topological p -wave pairing state exhibits non-Abelian statistics [18] and hence is useful for topological computation. In cold-atom experiments, a quasi-2D Fermi gas can be realized by arranging a one-dimensional optical lattice along the axial direction and a weak harmonic trapping

potential in the radial plane, such that fermions are strongly confined along the axial direction and form a series of pancake-shaped quasi-2D clouds [30–34].

For 2D fermionic systems with generic p - or d -wave pairing at zero temperature, the thermodynamic quantities and the velocity of the low-energy collective mode can be nonanalytic functions of the two-body binding energy at the BCS-BEC quantum phase transition point where the chemical potential vanishes [19,20,25]. Interestingly, these nonanalyticities are determined solely by the infrared behavior of the interaction potential, i.e., independent of the details of the interaction potential as well as the symmetry associated with the order parameter [25]. However, the temperature in a realistic ultracold-atomic gas is always nonzero. Therefore, it is important to study how these nonanalyticities are modified when the temperature is nonzero. In addition, it is well known that the thermal superfluid transition in 2D becomes of the Kosterlitz-Thouless (KT) type and vortex-antivortex lattice (VAL) may also exist at low temperature [35–37]. It is thus necessary to study the KT and VAL transitions in 2D fermionic systems with p - or d -wave pairing. The KT and VAL transitions has been comprehensively studied for 2D Fermi gases with s -wave pairing [8,38–44] and with spin-orbit coupling [45–49].

In this work, we present a systematical study of the KT and VAL melting transitions in 2D Fermi gases with p - or d -wave pairing. We find that the nonanalyticities are weakened by the finite-temperature effect. In particular, we calculate the sound velocity v as a function of temperature and interaction strength (the two-body binding energy). For the p -wave pairing, v is a nonmonotonous function of the two-body binding energy, while for the d -wave pairing, v decreases monotonously with the binding energy. The effect of mismatched Fermi surfaces is also studied for the d -wave pairing. In the BEC regime, we find that the KT and VAL transition temperatures both decrease linearly for large chemical potential imbalance, and a superfluid-normal phase transition occurs when the imbalance reaches a critical value.

The paper is arranged as follows. We present the study of a p -wave pairing system and a d -wave pairing system in Secs. II and III, respectively. The theoretical formalism is given in Secs. II A and III A. The numerical results are given in Sec. II B for p -wave pairing and in Sec. III B for d -wave pairing. Finally, we summarize in Sec. IV. We use the natural units $\hbar = k_B = 1$ throughout.

II. p -WAVE PAIRING IN SPINLESS FERMI GASES

A. Formalism in Gaussian approximation

Since the fermion wave function should be antisymmetric, the simplest setup to study p -wave pairing is a ‘‘spinless’’ Fermi gas, or single-component Fermi gas. The Hamiltonian can be written as [18,19]

$$\mathcal{H} = \sum_{\mathbf{k}} \xi_{\mathbf{k}} \psi_{\mathbf{k}}^{\dagger} \psi_{\mathbf{k}} + \sum_{\mathbf{k}, \mathbf{k}', \mathbf{q}} V_{\mathbf{k}\mathbf{k}'}^p b_{\mathbf{k}\mathbf{q}}^{\dagger} b_{\mathbf{k}'\mathbf{q}}, \quad (1)$$

where $\psi_{\mathbf{k}}$ represents the fermion annihilation operator, $b_{\mathbf{k}\mathbf{q}} = \psi_{-\mathbf{k}+\mathbf{q}/2} \psi_{\mathbf{k}+\mathbf{q}/2}$, and $\xi_{\mathbf{k}} = \epsilon_{\mathbf{k}} - \mu$ with the kinetic energy $\epsilon_{\mathbf{k}} = \mathbf{k}^2/(2m)$. For the sake of simplicity, we consider a separable

p -wave interaction potential $V_{\mathbf{k}\mathbf{k}'}^p$ [25],

$$V_{\mathbf{k}\mathbf{k}'}^p = -\lambda \Gamma^p(\mathbf{k}) \Gamma^{p*}(\mathbf{k}'), \quad (2)$$

where λ is the interaction strength. The Γ -functions takes the Nozières-Schmitt-Rink (NSR) form [3,19]

$$\Gamma_s^p(\mathbf{k}) = \frac{(k_x + ik_y)/k_1}{(1 + k/k_0)^{3/2}}, \quad \Gamma_a^p(\mathbf{k}) = \frac{k_x/k_1}{(1 + k/k_0)^{3/2}}, \quad (3)$$

with $k = |\mathbf{k}|$. Here, s and a represent the symmetric (isotropic) $p_x + ip_y$ and asymmetric (anisotropic) p_x pairings, respectively. The parameters k_0 and k_1 set the momentum scale in the short- and long-wavelength limits, respectively [19]. The form of the denominator is chosen to mimic the amplitude damping for p -wave partial potential at large momentum [19].

The partition function at finite temperature can be given by the imaginary-time path-integral formalism,

$$\mathcal{Z} = \int [d\psi^{\dagger}][d\psi] \exp \left\{ - \int_0^{\beta} d\tau \left(\sum_{\mathbf{k}} \psi_{\mathbf{k}}^{\dagger} \partial_{\tau} \psi_{\mathbf{k}} + \mathcal{H} \right) \right\}, \quad (4)$$

where $\tau = it$ is the imaginary time and $\beta = 1/T$, with T being the temperature. Introducing an auxiliary bosonic field $\phi_{\mathbf{q}}(\tau) = 2\lambda \sum_{\mathbf{k}} \Gamma^p(\mathbf{k}) b_{\mathbf{k}\mathbf{q}}$ and applying the Hubbard-Stratonovich transformation, we can rewrite the partition function as

$$\mathcal{Z} = \int [d\phi^*][d\phi][d\Psi^{\dagger}][d\Psi] \exp \left\{ - \int_0^{\beta} d\tau \left[\sum_{\mathbf{q}} \frac{|\phi_{\mathbf{q}}(\tau)|^2}{4\lambda} + \frac{1}{2} \sum_{\mathbf{k}, \mathbf{k}'} (\xi_{\mathbf{k}} \delta_{\mathbf{k}, \mathbf{k}'} - \Psi_{\mathbf{k}}^{\dagger} G_{\mathbf{k}, \mathbf{k}'}^{-1} \Psi_{\mathbf{k}'}) \right] \right\}, \quad (5)$$

where we use the Nambu-Gor'kov representation $\Psi_{\mathbf{k}}^{\dagger} = (\psi_{\mathbf{k}}^{\dagger}, \psi_{-\mathbf{k}})$. The inverse fermion Green's function is given by

$$G_{\mathbf{k}, \mathbf{k}'}^{-1}(\tau) = \begin{pmatrix} (-\partial_{\tau} - \xi_{\mathbf{k}}) \delta_{\mathbf{k}, \mathbf{k}'} & \phi_{\mathbf{k}-\mathbf{k}'}(\tau) \Gamma^p(\frac{\mathbf{k}+\mathbf{k}'}{2}) \\ \phi_{-\mathbf{k}+\mathbf{k}'}^*(\tau) \Gamma^{p*}(\frac{\mathbf{k}+\mathbf{k}'}{2}) & (-\partial_{\tau} + \xi_{\mathbf{k}}) \delta_{\mathbf{k}, \mathbf{k}'} \end{pmatrix}. \quad (6)$$

Integrating out the fermion degrees of freedom, we obtain

$$\mathcal{Z} = \int [d\phi^*][d\phi] e^{-\mathcal{S}_{\text{eff}}^p[\phi^*, \phi]}, \quad (7)$$

with the effective action

$$\mathcal{S}_{\text{eff}}^p = \int_0^{\beta} d\tau \left[\sum_{\mathbf{q}} \frac{|\phi_{\mathbf{q}}(\tau)|^2}{4\lambda} + \frac{1}{2} \sum_{\mathbf{k}, \mathbf{k}'} (\xi_{\mathbf{k}} \delta_{\mathbf{k}, \mathbf{k}'} - \text{Tr} \ln G_{\mathbf{k}, \mathbf{k}'}^{-1}) \right], \quad (8)$$

where the trace is taken over imaginary time, momentum, and Nambu-Gor'kov spaces.

To proceed, we decompose the auxiliary field $\phi_{\mathbf{q}}(\tau)$ into its mean-field and fluctuation parts,

$$\phi_{\mathbf{q}}(\tau) = \Delta \delta_{\mathbf{q}, \mathbf{0}} + \hat{\phi}_{\mathbf{q}}(\tau). \quad (9)$$

The effective action can be evaluated in powers of the fluctuation $\hat{\phi}_{\mathbf{q}}(\tau)$, i.e., $\mathcal{S}_{\text{eff}}^p = \mathcal{S}_0^p + \mathcal{S}_2^p + \dots$. Here we omit the linear term in the fluctuation since it vanishes due to the gap equation. The leading-order term \mathcal{S}_0^p represents the mean-field contribution. The next-to-leading-order term \mathcal{S}_2^p , which is quadratic in the fluctuation, represents the Gaussian fluctuations and hence the collective mode dynamics.

1. Mean-field approximation

The mean-field contribution \mathcal{S}_0^p can be evaluated as

$$\mathcal{S}_0^p = \beta S \left[\frac{\Delta^2}{4\lambda} + \frac{1}{2} \int \frac{d^2\mathbf{k}}{(2\pi)^2} \xi_{\mathbf{k}} - \frac{T}{2} \sum_n \int \frac{d^2\mathbf{k}}{(2\pi)^2} \ln \det \mathcal{G}_{\mathbf{k}}^{-1}(i\omega_n) \right] = \beta S \left\{ \frac{\Delta^2}{4\lambda} - \frac{1}{2} \int \frac{d^2\mathbf{k}}{(2\pi)^2} [E_{\mathbf{k}} - \xi_{\mathbf{k}} + 2T \ln(1 + e^{-E_{\mathbf{k}}/T})] \right\}, \quad (10)$$

where S is the area of the system and $\omega_n = (2n + 1)\pi T$ ($n \in \mathbb{Z}$) is the fermion Matsubara frequency. The inverse fermion Green's function in the mean-field approximation is given by

$$\mathcal{G}_{\mathbf{k}}^{-1}(i\omega_n) = \begin{pmatrix} i\omega_n - \xi_{\mathbf{k}} & \Delta_{\mathbf{k}}^{\text{p}} \\ \Delta_{\mathbf{k}}^{\text{p}*} & i\omega_n + \xi_{\mathbf{k}} \end{pmatrix}, \quad (11)$$

which gives the fermionic quasiparticle spectrum $E_{\mathbf{k}} = (\xi_{\mathbf{k}}^2 + |\Delta_{\mathbf{k}}^{\text{p}}|^2)^{1/2}$ with $\Delta_{\mathbf{k}}^{\text{p}} = \Delta \Gamma^{\text{p}}(\mathbf{k})$. The mean field Δ , normally referred to as the superfluid order parameter, is determined by the extreme condition $\partial \mathcal{S}_0^{\text{p}} / \partial \Delta = 0$, which gives rise to the gap equation

$$\frac{1}{\lambda} = \int \frac{d^2\mathbf{k}}{(2\pi)^2} \frac{|\Gamma^{\text{p}}(\mathbf{k})|^2}{E_{\mathbf{k}}} \tanh\left(\frac{E_{\mathbf{k}}}{2T}\right). \quad (12)$$

The mean-field contribution to the number density is obtained through the thermodynamic relation $n_0 = -(\partial \mathcal{S}_0^{\text{p}} / \partial \mu) / (\beta S)$. We have

$$n_0 \equiv \int \frac{d^2\mathbf{k}}{(2\pi)^2} n_0(\mathbf{k}) = \frac{1}{2} \int \frac{d^2\mathbf{k}}{(2\pi)^2} \left[1 - \frac{\xi_{\mathbf{k}}}{E_{\mathbf{k}}} \tanh\left(\frac{E_{\mathbf{k}}}{2T}\right) \right]. \quad (13)$$

The interaction strength λ can be physically characterized by the two-body binding energy E_b in vacuum. It is given by [19]

$$\frac{1}{\lambda} = \int \frac{d^2\mathbf{k}}{(2\pi)^2} \frac{2|\Gamma^{\text{p}}(\mathbf{k})|^2}{2\epsilon_{\mathbf{k}} - E_b}. \quad (14)$$

Note that unlike the s -wave case, here the binding energy E_b can be both negative or positive. The weak and strong attraction limits correspond to $E_b \rightarrow +\infty$ and $E_b \rightarrow -\infty$, respectively.

2. Gaussian fluctuation and Goldstone mode

The Gaussian fluctuation contribution to the effective action is quadratic in $\phi_{\mathbf{q}}(\tau)$ and thus represents the collective mode

dynamics. It can be evaluated as

$$\mathcal{S}_2^{\text{p}} = \sum_{\mathbf{q}, n} \left\{ \frac{|\hat{\phi}_{\mathbf{q}}(i\nu_n)|^2}{4\lambda} + \frac{T}{4S} \sum_{\mathbf{k}, m} \text{Tr}[\mathcal{G}_{\mathbf{k}-\mathbf{q}/2}(i\omega_m) \times \Phi_{-\mathbf{q}}(-i\nu_n) \mathcal{G}_{\mathbf{k}+\mathbf{q}/2}(i\omega_m + i\nu_n) \Phi_{\mathbf{q}}(i\nu_n)] \right\}, \quad (15)$$

where $\nu_n = 2\pi n T$ ($n \in \mathbb{Z}$) is the boson Matsubara frequency, and the mean-field fermion Green's function and the vertex matrix Φ are given by

$$\mathcal{G}_{\mathbf{k}}(i\omega_m) = \frac{1}{(i\omega_m)^2 - E_{\mathbf{k}}^2} \begin{pmatrix} (i\omega_m + \xi_{\mathbf{k}}) & -\Delta_{\mathbf{k}}^{\text{p}} \\ -\Delta_{\mathbf{k}}^{\text{p}*} & (i\omega_m - \xi_{\mathbf{k}}) \end{pmatrix},$$

$$\Phi_{\mathbf{q}}(i\nu_n) = \begin{pmatrix} 0 & \hat{\phi}_{\mathbf{q}}(i\nu_n) \Gamma^{\text{p}}(\mathbf{k}) \\ \hat{\phi}_{-\mathbf{q}}^*(i\nu_n) \Gamma^{\text{p}*}(\mathbf{k}) & 0 \end{pmatrix}. \quad (16)$$

After some algebra, \mathcal{S}_2^{p} can be written in a compact form,

$$\mathcal{S}_2^{\text{p}} = \frac{1}{2} \sum_{\mathbf{q}, n} [\hat{\phi}_{\mathbf{q}}^*(i\nu_n) \hat{\phi}_{-\mathbf{q}}(-i\nu_n)] M(\mathbf{q}, i\nu_n) \begin{pmatrix} \hat{\phi}_{\mathbf{q}}(i\nu_n) \\ \hat{\phi}_{-\mathbf{q}}^*(-i\nu_n) \end{pmatrix}, \quad (17)$$

where the inverse boson propagator $M(\mathbf{q}, i\nu_n)$ takes the form

$$M(\mathbf{q}, i\nu_n) = \begin{pmatrix} M_{11}(\mathbf{q}, i\nu_n) & M_{12}(\mathbf{q}, i\nu_n) \\ M_{21}(\mathbf{q}, i\nu_n) & M_{22}(\mathbf{q}, i\nu_n) \end{pmatrix}. \quad (18)$$

The matrix elements are given by

$$M_{11} = \frac{1}{4\lambda} + \frac{T}{2S} \sum_{\mathbf{k}, m} \mathcal{G}_{\mathbf{k}-\mathbf{q}/2}^{11}(i\omega_m) \mathcal{G}_{\mathbf{k}+\mathbf{q}/2}^{22}(i\omega_m + i\nu_n) |\Gamma^{\text{p}}(\mathbf{k})|^2,$$

$$M_{22} = \frac{1}{4\lambda} + \frac{T}{2S} \sum_{\mathbf{k}, m} \mathcal{G}_{\mathbf{k}-\mathbf{q}/2}^{22}(i\omega_m) \mathcal{G}_{\mathbf{k}+\mathbf{q}/2}^{11}(i\omega_m + i\nu_n) |\Gamma^{\text{p}}(\mathbf{k})|^2,$$

$$M_{12} = \frac{T}{2S} \sum_{\mathbf{k}, m} \mathcal{G}_{\mathbf{k}-\mathbf{q}/2}^{12}(i\omega_m) \mathcal{G}_{\mathbf{k}+\mathbf{q}/2}^{12}(i\omega_m + i\nu_n) [\Gamma^{\text{p}*}(\mathbf{k})]^2,$$

$$M_{21} = \frac{T}{2S} \sum_{\mathbf{k}, m} \mathcal{G}_{\mathbf{k}-\mathbf{q}/2}^{21}(i\omega_m) \mathcal{G}_{\mathbf{k}+\mathbf{q}/2}^{21}(i\omega_m + i\nu_n) [\Gamma^{\text{p}}(\mathbf{k})]^2. \quad (19)$$

It is easy to prove that these matrix elements satisfy

$$M_{11}^*(\mathbf{q}, i\nu_n) = M_{22}(\mathbf{q}, i\nu_n), \quad M_{12}^*(\mathbf{q}, i\nu_n) = M_{21}(\mathbf{q}, i\nu_n). \quad (20)$$

Completing the fermion Matsubara frequency summation, we obtain

$$M_{11} = \frac{1}{4\lambda} + \int \frac{d^2\mathbf{k}}{(2\pi)^2} \frac{|\Gamma^{\text{p}}(\mathbf{k})|^2}{2} \left\{ \left[\frac{u_-^2 v_+^2}{i\nu_n + (E_+ - E_-)} - \frac{u_+^2 v_-^2}{i\nu_n - (E_+ - E_-)} \right] (f_+ - f_-) \right.$$

$$\left. + \left[\frac{u_+^2 u_-^2}{i\nu_n - (E_+ + E_-)} - \frac{v_+^2 v_-^2}{i\nu_n + (E_+ + E_-)} \right] (1 - f_+ - f_-) \right\},$$

$$M_{12} = - \int \frac{d^2\mathbf{k}}{(2\pi)^2} \frac{[\Gamma^{\text{p}*}(\mathbf{k})]^2}{8E_+ E_-} \left\{ \left[\frac{\Delta_{\mathbf{k}-\mathbf{q}/2}^{\text{p}} \Delta_{\mathbf{k}+\mathbf{q}/2}^{\text{p}}}{i\nu_n - (E_+ - E_-)} - \frac{\Delta_{\mathbf{k}-\mathbf{q}/2}^{\text{p}} \Delta_{\mathbf{k}+\mathbf{q}/2}^{\text{p}}}{i\nu_n + (E_+ - E_-)} \right] (f_+ - f_-) \right.$$

$$\left. + \left[\frac{\Delta_{\mathbf{k}-\mathbf{q}/2}^{\text{p}} \Delta_{\mathbf{k}+\mathbf{q}/2}^{\text{p}}}{i\nu_n - (E_+ + E_-)} - \frac{\Delta_{\mathbf{k}-\mathbf{q}/2}^{\text{p}} \Delta_{\mathbf{k}+\mathbf{q}/2}^{\text{p}}}{i\nu_n + (E_+ + E_-)} \right] (1 - f_+ - f_-) \right\}, \quad (21)$$

where the BCS distributions are defined as $u_{\pm}^2 = (1 + \xi_{\pm}/E_{\pm})/2$ and $v_{\pm}^2 = (1 - \xi_{\pm}/E_{\pm})/2$, and the Fermi-Dirac distribution is given by $f_{\pm} = (1 + e^{E_{\pm}/T})^{-1}$, with the dispersions $\xi_{\pm} = \xi_{\mathbf{k}\pm\mathbf{q}/2}$ and $E_{\pm} = E_{\mathbf{k}\pm\mathbf{q}/2}$. We note that the terms proportional to $f_+ - f_-$ correspond to the Landau damping effect, which vanish when $T \rightarrow 0$.

It is more physical to decompose the fluctuation into its real and imaginary parts, i.e., $\hat{\phi}(x) = \sigma(x) + i\pi(x)$. In momentum space, we have $\hat{\phi}_{\mathbf{q}}(i\nu_n) = \sigma_{\mathbf{q}}(i\nu_n) + i\pi_{\mathbf{q}}(i\nu_n)$ and $\hat{\phi}_{\mathbf{q}}^*(i\nu_n) = \sigma_{\mathbf{q}}^*(i\nu_n) - i\pi_{\mathbf{q}}^*(i\nu_n) = \sigma_{-\mathbf{q}}(-i\nu_n) - i\pi_{-\mathbf{q}}(-i\nu_n)$. Thus, the Gaussian fluctuation part of the effective action can be expressed as

$$S_2^p = \frac{1}{2} \sum_{\mathbf{q},n} [\sigma_{\mathbf{q}}^*(i\nu_n) \quad \pi_{\mathbf{q}}^*(i\nu_n)] \Pi(\mathbf{q}, i\nu_n) \begin{pmatrix} \sigma_{\mathbf{q}}(i\nu_n) \\ \pi_{\mathbf{q}}(i\nu_n) \end{pmatrix}, \quad (22)$$

where the inverse boson propagator reads

$$\Pi = \begin{pmatrix} (M_{11} + M_{12} + M_{21} + M_{22}) & i(-M_{11} - M_{12} + M_{21} + M_{22}) \\ i(M_{11} - M_{12} + M_{21} - M_{22}) & (M_{11} - M_{12} - M_{21} + M_{22}) \end{pmatrix}. \quad (23)$$

The low-energy dynamics is governed by the gapless Goldstone mode. Diagonalizing the matrix Π , we obtain two eigenmodes. Their inverse propagators are given by

$$\mathcal{D}_{\theta/\eta}^{-1}(\mathbf{q}, i\nu_n) = M_{11} + M_{22} \mp \sqrt{(M_{11} - M_{22})^2 + 4M_{12}M_{21}}. \quad (24)$$

We can prove that $\mathcal{D}_{\theta}^{-1}(\mathbf{0}, 0) = 0$, which indicates that the θ mode is gapless, i.e., the Goldstone mode. It is a mixture of σ and π components and can be expressed as

$$\theta_{\mathbf{q}}(i\nu_n) = C[\mathcal{D}_{\theta}^{-1}(\mathbf{q}, i\nu_n)\sigma_{\mathbf{q}}(i\nu_n) + \mathcal{D}_{\eta}^{-1}(\mathbf{q}, i\nu_n)\pi_{\mathbf{q}}(i\nu_n)], \quad (25)$$

where C is a normalization coefficient.

The KT transition is related to the stiffness of the Goldstone mode, i.e., the gapless θ mode. To this end, we need to study the low-energy dynamics of the collective modes. At small energy and momentum, the propagator of the gapless θ mode can be expressed as

$$\mathcal{D}_{\theta}^{-1}(\mathbf{q}, i\nu_n) = -\zeta^p(i\nu_n)^2 + \frac{1}{4m\Delta^2}(\rho_x^p q_x^2 + \rho_y^p q_y^2), \quad (26)$$

where ρ_x^p and ρ_y^p are the so-called stiffnesses of the Goldstone mode. To compute the coefficients ζ^p , ρ_x^p , and ρ_y^p , we make the low-energy expansion of M_{ij} ($i, j = 1, 2$) to the quadratic order in frequency and momentum,

$$M_{ij}(\mathbf{q}, i\nu_n) = A_{ij} + i\nu_n B_{ij} + (i\nu_n)^2 C_{ij} + D_{ij}^x q_x^2 + D_{ij}^y q_y^2. \quad (27)$$

However, because of the Landau damping terms proportional to $f_+ - f_-$ in Eq. (21), such an expansion is, in principle, only valid at zero temperature or near the superfluid transition temperature [5,50]. Mathematically, the Landau damping terms bring divergences when doing such an expansion. Since the KT and VAL melting transitions occur at low temperature where the pairing gap is still large, we may neglect the divergences from the Landau damping effect and perform this expansion. Physically, in this approximation, we neglect the damping of the collective modes and treat them as stable modes. Below the KT transition temperature, we expect that the large pairing gap suppresses the damping of the collective modes and validates this approximation.

By neglecting the Landau damping effect, we can evaluate the expansion coefficients as

$$\begin{aligned} A_{11} = A_{22} &= \frac{1}{4\lambda} - \int \frac{d^2\mathbf{k}}{(2\pi)^2} (E_{\mathbf{k}}^2 + \xi_{\mathbf{k}}^2) \frac{|\Gamma^p(\mathbf{k})|^2}{8E_{\mathbf{k}}^3} \tanh\left(\frac{E_{\mathbf{k}}}{2T}\right), \\ B_{11} = -B_{22} &= - \int \frac{d^2\mathbf{k}}{(2\pi)^2} \frac{\xi_{\mathbf{k}} |\Gamma^p(\mathbf{k})|^2}{8E_{\mathbf{k}}^3} \tanh\left(\frac{E_{\mathbf{k}}}{2T}\right), \\ C_{11} = C_{22} &= - \int \frac{d^2\mathbf{k}}{(2\pi)^2} (E_{\mathbf{k}}^2 + \xi_{\mathbf{k}}^2) \frac{|\Gamma^p(\mathbf{k})|^2}{32E_{\mathbf{k}}^5} \tanh\left(\frac{E_{\mathbf{k}}}{2T}\right), \\ A_{12} = A_{21} &= \Delta^2 \int \frac{d^2\mathbf{k}}{(2\pi)^2} \frac{|\Gamma^p(\mathbf{k})|^4}{8E_{\mathbf{k}}^3} \tanh\left(\frac{E_{\mathbf{k}}}{2T}\right), \\ B_{12} = B_{21} &= 0, \\ C_{12} = C_{21} &= \Delta^2 \int \frac{d^2\mathbf{k}}{(2\pi)^2} \frac{|\Gamma^p(\mathbf{k})|^4}{32E_{\mathbf{k}}^5} \tanh\left(\frac{E_{\mathbf{k}}}{2T}\right). \end{aligned} \quad (28)$$

The coefficients $D_{ij}^{x,y}$ can be obtained, but are quite lengthy (see the Appendix). Here we show the combined quantities,

$$\rho_i^p = 4m\Delta^2(D_{11}^i + D_{22}^i - D_{12}^i - D_{21}^i), \quad i = x, y, \quad (29)$$

which are exactly the superfluid density along the x and y directions. After a lengthy calculation, we obtain

$$\rho_i^p = \int \frac{d^2\mathbf{k}}{(2\pi)^2} \left[n_0(\mathbf{k}) - \frac{k_i^2}{4mT} \operatorname{sech}^2\left(\frac{E_{\mathbf{k}}}{2T}\right) \right]. \quad (30)$$

At zero temperature, the superfluid density is isotropic for both p_x and $p_x + ip_y$ pairings and we have $\rho_x^p = \rho_y^p = n$ as required by the Galilean invariance [51,52]. However, for p_x pairing, the finite-temperature effect generates anisotropy of the superfluid density.

Finally, the low-energy behavior of the θ mode or the Goldstone mode is given by Eq. (26), where the coefficient ζ^p reads

$$\zeta^p = \zeta_0^p + \frac{B_{11}^2}{A_{12}}, \quad (31)$$

with $\zeta_0^p = -2(C_{11} - C_{12})$. The Goldstone mode velocity or sound velocity along the i direction reads

$$v_i^p = \sqrt{\frac{\rho_i^p}{4m\Delta^2\zeta^p}}. \quad (32)$$

We note that the term B_{11}^2/A_{12} arises from the coupling between the phase and amplitude modes and is rather important to recover the correct sound velocity in the BCS-BEC evolution [43]. We also emphasize that even though the low-energy expansion of the matrix elements $M_{ij}(\mathbf{q}, i\nu_n)$ suffers from the divergence problem caused by the Landau damping effect, these divergences cancel exactly for the coefficients ζ^p , ρ_x^p , and ρ_y^p . The divergences only arise for higher-order terms in the expansion (26). These divergences correspond to the damping of the Goldstone mode and we may neglect it at low temperature.

Comparing to the previous approach to the KT transition in superfluid 2D Fermi gases [8,40,53], we make some comments here. The previous approach adopted an alternative decomposition of the superfluid order parameter field $\phi(x)$, i.e., $\phi(x) = [\Delta + \eta(x)]e^{i\theta(x)}$, and the amplitude fluctuation $\eta(x)$ is normally neglected [8,40,53]. The KT transition can be obtained by studying the low-energy dynamics of the pure phase mode $\theta(x)$. The advantage of this approach is that it formally does not suffer from the Landau damping problem, as we encounter here. We have also evaluated the low-energy expansion for the phase mode in this approach. The expansion also takes the form (26) and leads to the same result for the superfluid density ρ_i^p . However, the coefficient ζ^p is different [53]:

$$\zeta^p = \int \frac{d^2\mathbf{k}}{(2\pi)^2} \frac{|\Gamma^p(\mathbf{k})|^2}{8E_{\mathbf{k}}^2} \times \left[\frac{|\Delta_{\mathbf{k}}^p|^2}{E_{\mathbf{k}}} \tanh\left(\frac{E_{\mathbf{k}}}{2T}\right) + \frac{\xi_{\mathbf{k}}^2}{2T} \operatorname{sech}^2\left(\frac{E_{\mathbf{k}}}{2T}\right) \right]. \quad (33)$$

We can easily identify that the first term is just ζ_0^p and the second term comes from the fact that this approach amounts to take the limit $\mathbf{q} \rightarrow 0$ first when evaluating the low-energy expansion. As clarified in [43], this approach leads to an incorrect result for the sound velocity v_i^p in the BCS-BEC evolution. In summary, our approach can recover not only the correct superfluid density but also the correct sound velocity. The price we pay in this approach is that we have to neglect the damping of the collective modes.

In our low-energy approximation, the contribution of the Goldstone mode to the thermodynamic potential can be given by

$$\Omega_2^p = \int \frac{d^2\mathbf{q}}{(2\pi)^2} T \ln(1 - e^{-\varepsilon_{\mathbf{q}}/T}) = -\frac{\zeta(3)T^3}{2\pi(v_x^p v_y^p)}, \quad (34)$$

where the dispersion relation of the Goldstone mode is given by $\varepsilon_{\mathbf{q}} = [\sum_{i=x,y} (v_i^p q_i)^2]^{1/2}$ and $\zeta(x)$ is the Riemann zeta function. At finite temperature, we take into account the fluctuation contribution to the number density. The total fermion number density n can be given by

$$n = n_0 - \frac{\partial \Omega_2^p}{\partial \mu} = n_0 - \frac{\zeta(3)T^3}{2\pi(v_x^p v_y^p)^2} \frac{\partial (v_x^p v_y^p)}{\partial \mu}. \quad (35)$$

At $T = 0$, we have $n = n_0$ and therefore the quantum fluctuations [54–56] are not taken into account in the present theory. For s -wave pairing, it was found that inclusion of quantum fluctuations leads to slight correction to the KT transition [57,58]. Thus we expect that the present theory can provides

reliable results for the KT and VAL transition for higher partial wave pairings.

B. Kosterlitz-Thouless and vortex-antivortex lattice melting transitions

The KT and VAL melting temperatures are both directly related to the stiffness $J_i = \rho_i^p/(4m)$ [35–37,53],

$$T_{\text{KT}} = \frac{\pi}{2} \sqrt{J_x^p(T_{\text{KT}})J_y^p(T_{\text{KT}})}, \quad T_{\text{M}} = 0.3 \sqrt{J_x^p(T_{\text{M}})J_y^p(T_{\text{M}})}. \quad (36)$$

For the anisotropic p_x pairing, the vortex might be elliptically shaped and the usual square vortex-antivortex lattice will also deform accordingly, just like the case with anisotropic spin-orbit coupling [46]. However, one can scale one direction so that the scaled vortex is circular (the scaled lattice thus becomes square). Thus we can apply Eq. (36) to the scaled vortex and lattice. Then for a given E_b and number density, the gap equation (12), the number equation (35), and the critical temperature equation (36) can be solved self-consistently to give $T_{\text{KT}}(T_{\text{M}})$ and Δ and μ at $T_{\text{KT}}(T_{\text{M}})$.

To present the numerical results, it is convenient to define the Fermi momentum k_{F} and Fermi energy ϵ_{F} of a noninteracting Fermi gas, through $n = k_{\text{F}}^2/(4\pi)$ and $\epsilon_{\text{F}} = k_{\text{F}}^2/(2m)$. The numerical results are shown in Fig. 1 in which we plot the transition temperatures T_{KT} and T_{M} , the chemical potential, the order parameter, and the sound velocity at T_{KT} and T_{M} as functions of E_b . The E_b dependence of T_{KT} clearly shows the BCS-BEC evolution when E_b is tuned from positive to negative values (note that for p -wave pairing in 2D, an attractive potential does not necessarily lead to a bound state; when $E_b > 0$, the two-fermion state is a scattering state). The chemical potential at T_{KT} and T_{M} is almost the same for a given p -wave pairing; similarly, the order parameter at T_{KT} and T_{M} is also almost the same. In the deep BEC region where $E_b < 0$ with a large magnitude, the transition temperatures T_{KT} and T_{M} are found to be constants, $T_{\text{KT}} \simeq 0.0625\epsilon_{\text{F}}$ and $T_{\text{M}} \simeq (0.6/\pi)T_{\text{KT}}$, which are comparable to the s -wave pairing case [53]. In addition, the anisotropy in the sound velocity disappears for p_x pairing in the deep BEC region, as illuminated in the plot of the sound velocities v_x and v_y , because the basic degrees of freedom are now compactly bound bosons and the Yoshida term in Eq. (30) is suppressed.

One interesting feature that we observe is that there is nonanalytic behavior at the BCS-BEC transition point $\mu = 0$. We can see this most clearly from the sound velocity. For other values of μ , the KT and VAL melting transitions are always analytic and smooth. To illuminate this more explicitly, we show the results for T_{KT} around the region $\mu \sim 0$ in one of the insets of Fig. 1 for the anisotropic p_x pairing, which is more obvious than the isotropic $p_x + ip_y$ pairing. In order to understand the nonanalyticity, we explore the properties of the most relevant quantity ζ_0^p around $\mu = 0$. The first two derivatives of ζ_0^p with respect to μ are given by

$$\frac{\partial \zeta_0^p}{\partial \mu} = \int \frac{d^2\mathbf{k}}{(2\pi)^2} \frac{\xi_{\mathbf{k}} |\Gamma^p(\mathbf{k})|^2}{8E_{\mathbf{k}}^4} \left[\frac{3 \tanh\left(\frac{E_{\mathbf{k}}}{2T}\right)}{E_{\mathbf{k}}} - \frac{\operatorname{sech}^2\left(\frac{E_{\mathbf{k}}}{2T}\right)}{2T} \right], \quad (37)$$

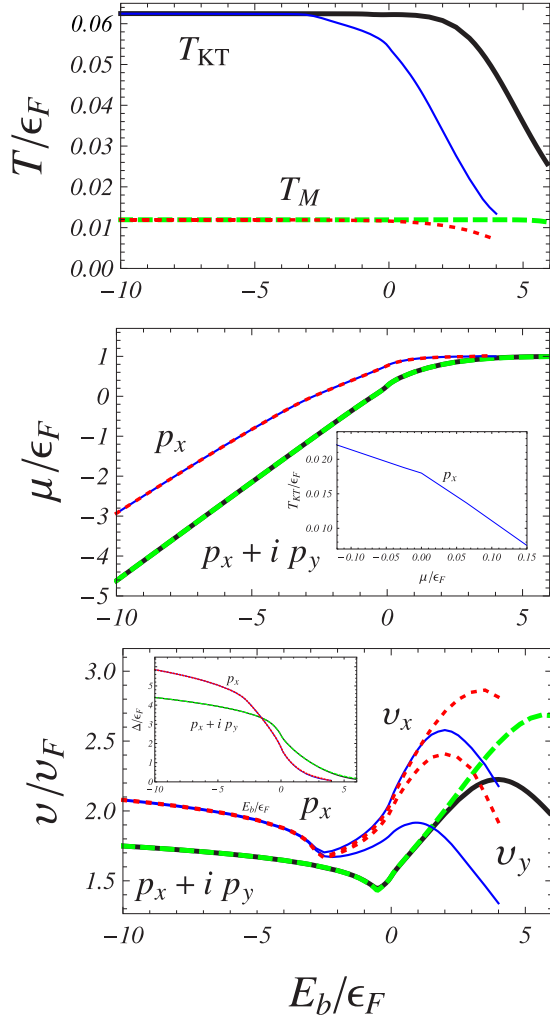


FIG. 1. Upper panel: The transition temperatures, T_{KT} (solid lines) and T_M (dashed lines), as functions of the two-body binding energy E_b for the isotropic $p_x + ip_y$ pairing (black and green thick lines) and anisotropic p_x pairing (blue and red thin lines). Lower panels: The chemical potential μ and sound velocity v as functions of E_b at T_{KT} and T_M . The anisotropic velocities for p_x pairing are denoted by v_x and v_y . The insets show the zoom-in plots of T_{KT} with respect to μ around the BCS-BEC transition point $\mu = 0$ for the p_x pairing and the order parameter Δ as a function of E_b . The parameters for the NSR potential are $k_0 = 10^{3/2}k_F$ and $k_1 = 10^{1/2}k_F$.

$$\begin{aligned} \frac{\partial^2 \zeta_0^P}{\partial \mu^2} = & \int \frac{d^2 \mathbf{k}}{(2\pi)^2} \frac{|\Gamma^P(\mathbf{k})|^2}{8E_{\mathbf{k}}^5} \left[\frac{3(5\xi_{\mathbf{k}}^2 - E_{\mathbf{k}}^2)}{E_{\mathbf{k}}^2} \tanh\left(\frac{E_{\mathbf{k}}}{2T}\right) \right. \\ & - \frac{|\Delta_{\mathbf{k}}^P|^2}{2TE_{\mathbf{k}}} \operatorname{sech}^2\left(\frac{E_{\mathbf{k}}}{2T}\right) \\ & \left. - \frac{\xi_{\mathbf{k}}^2}{2T^2} \tanh\left(\frac{E_{\mathbf{k}}}{2T}\right) \operatorname{sech}^2\left(\frac{E_{\mathbf{k}}}{2T}\right) \right]. \end{aligned} \quad (38)$$

For small $\mu \rightarrow 0^+$, $\partial \zeta_0^P / \partial \mu$ is finite but

$$\frac{\partial^2 \zeta_0^P}{\partial \mu^2} \sim \frac{1}{T \Delta^4} \ln \frac{\mu}{\Delta}. \quad (39)$$

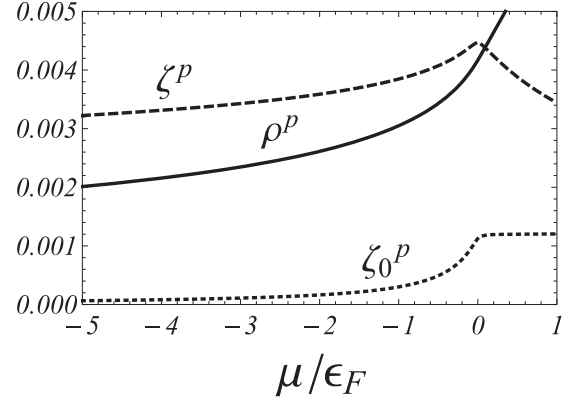


FIG. 2. The behavior of the quantities ζ_0^P , ζ^P , and ρ^P with respect to the chemical potential μ for the $p_x + ip_y$ pairing. These quantities have been scaled by proper constants so that they are dimensionless in the plot. In the calculations, we choose $T = 0.06\epsilon_F$ and $\Delta = 4\epsilon_F$. The parameters for the NSR potential are the same as used in Fig. 1.

As ζ_0^P appears in n and ρ_i^P , this shows that the higher-order derivatives of n and ρ_i^P with respect to μ are not analytic at the point where $\mu = 0$. Also, T_{KT} , T_M , and the sound velocity v are all nonanalytic at the point where $\mu = 0$. But we note that the temperature effect weakens the nonanalyticities, as can be seen from the above equations. Thus, the BCS-BEC evolution in the p -wave pairing system is actually a phase transition, although there is no change of symmetry across the transition.

The sound velocities behave nonmonotonically versus E_b and we will analyze it in more detail. For the anisotropic p_x pairing, the sound velocities along the x and y directions split in the BCS region (E_b positive and large) and merge into a single curve in the deep BEC region. For the isotropic $p_x + ip_y$ pairing, we plot the relevant functions ζ_0^P , ζ^P , and ρ^P versus the chemical potential μ in Fig. 2 to understand the extremas in the sound velocities. As can be seen, the term B_{11}^2/A_{12} dominates ζ_0^P at low temperature, which indicates the importance of the σ component in the θ mode and the increasing feature of the sound velocities in the BCS region is due to the fast decreasing of ζ^P . The sound velocity decreases in the BCS regime with large E_b where Δ is small. This interesting nonmonotonic behavior of the sound velocity may be used to probe the BCS-BEC transition in Fermi gases with p -wave pairing.

III. d -WAVE PAIRING IN SPIN-1/2 FERMI GASES

A. Formalism in Gaussian approximation

We now consider a spin-1/2 Fermi gas or a two-component Fermi gas with a d -wave interaction between the unlike spin components. In this case, Fermi surface mismatch between different spin components can be introduced through the Zeeman effect induced by a magnetic field [59–62], through imbalance spin populations [63–65] or through spin-orbit coupling [66]. The Hamiltonian density can be written as [20]

$$\mathcal{H} = \sum_{\mathbf{k}, s=\uparrow\downarrow} \xi_{\mathbf{k}s} \psi_{\mathbf{k},s}^\dagger \psi_{\mathbf{k},s} + \sum_{\mathbf{k}, \mathbf{k}', q} V_{\mathbf{k}\mathbf{k}'}^d b_{\mathbf{k}q}^\dagger b_{\mathbf{k}'q}, \quad (40)$$

where $\psi_{\mathbf{k},s}$ represents the fermion annihilation operator with spin $s = \uparrow, \downarrow$, $b_{\mathbf{k}\mathbf{q}} = \psi_{-\mathbf{k}+\mathbf{q}/2, \downarrow} \psi_{\mathbf{k}+\mathbf{q}/2, \uparrow}$, and $\xi_{\mathbf{k}s} = \xi_{\mathbf{k}} - s\delta\mu$. Here and in the following, $s = +(-)$ for the spin $\uparrow(\downarrow)$ is used. For the sake of simplicity, we consider a separable d -wave interaction potential [25],

$$V_{\mathbf{k}\mathbf{k}'}^d = -\lambda \Gamma^d(\mathbf{k}) \Gamma^{d*}(\mathbf{k}'), \quad (41)$$

where the Γ -functions are defined according to NSR-type potentials [19],

$$\begin{aligned} \Gamma_s^d(\mathbf{k}) &= \frac{(k_x + ik_y)^2/k_1^2}{(1 + k/k_0)^{5/2}}, \\ \Gamma_a^d(\mathbf{k}) &= \frac{(k_x^2 - k_y^2)/k_1^2}{(1 + k/k_0)^{5/2}}, \end{aligned} \quad (42)$$

with s and a representing the symmetric (or isotropic) $d_{x^2-y^2} + 2id_{xy}$ and asymmetric (or anisotropic) $d_{x^2-y^2}$ pairings, respectively. The form of the denominator is chosen to mimic the amplitude damping for d -wave partial potential at large momentum [19].

Then, the partition function at finite temperature is given by

$$\begin{aligned} \mathcal{Z} &= \int \prod_{s=\uparrow\downarrow} [d\psi_s^\dagger][d\psi_s] \\ &\times \exp \left\{ - \int_0^\beta d\tau \left(\sum_{\mathbf{k}, s=\uparrow\downarrow} \psi_{\mathbf{k},s}^\dagger \partial_\tau \psi_{\mathbf{k},s} + \mathcal{H} \right) \right\}. \end{aligned} \quad (43)$$

Introducing the auxiliary field $\phi_{\mathbf{q}}(\tau) = \lambda \sum_{\mathbf{k}} \Gamma^d(\mathbf{k}) b_{\mathbf{k}\mathbf{q}}$ through Hubbard-Stratonovich transformation, the partition function can be rewritten as

$$\begin{aligned} \mathcal{Z} &= \int [d\phi^*][d\phi][d\Psi^\dagger][d\Psi] \exp \left\{ - \int_0^\beta d\tau \left[\sum_{\mathbf{k}} \frac{|\phi_{\mathbf{k}}(\tau)|^2}{\lambda} \right. \right. \\ &\left. \left. + \sum_{\mathbf{k}, \mathbf{k}'} (\xi_{\mathbf{k}} \delta_{\mathbf{k}, \mathbf{k}'} + \Psi_{\mathbf{k}}^\dagger G_{\mathbf{k}, \mathbf{k}'}^{-1} \Psi_{\mathbf{k}'}) \right] \right\}, \end{aligned} \quad (44)$$

where the fermion field in Nambu-Gor'kov space is $\Psi_{\mathbf{k}}^\dagger = (\psi_{\mathbf{k}, \uparrow}^\dagger, \psi_{-\mathbf{k}, \downarrow})$. The inverse propagator is then a 2×2 matrix, which is given by

$$G_{\mathbf{k}, \mathbf{k}'}^{-1}(\tau) = \begin{pmatrix} (\partial_\tau + \xi_{\mathbf{k}\uparrow}) \delta_{\mathbf{k}, \mathbf{k}'} & -\phi_{\mathbf{k}-\mathbf{k}'}(\tau) \Gamma^d(\frac{\mathbf{k}+\mathbf{k}'}{2}) \\ -\phi_{-\mathbf{k}+\mathbf{k}'}^*(\tau) \Gamma^{d*}(\frac{\mathbf{k}+\mathbf{k}'}{2}) & (\partial_\tau - \xi_{\mathbf{k}\downarrow}) \delta_{\mathbf{k}, \mathbf{k}'} \end{pmatrix}. \quad (45)$$

Integrating out the fermion degrees of freedom, we can get a bosonic version of the partition function,

$$\mathcal{Z} = \int [d\phi^*][d\phi] e^{-\mathcal{S}_{\text{eff}}^d[\phi^*, \phi]}, \quad (46)$$

with the effective action

$$\mathcal{S}_{\text{eff}}^d = \int_0^\beta d\tau \left[\sum_{\mathbf{k}} \frac{|\phi_{\mathbf{k}}(\tau)|^2}{\lambda} + \sum_{\mathbf{k}, \mathbf{k}'} (\xi_{\mathbf{k}} \delta_{\mathbf{k}, \mathbf{k}'} - \text{Tr} \ln G_{\mathbf{k}, \mathbf{k}'}^{-1}) \right], \quad (47)$$

where the trace is taken over imaginary time, momentum, and Nambu-Gorkov spaces.

To proceed, we decompose the auxiliary field $\phi_{\mathbf{q}}(\tau)$ into its mean-field and fluctuation parts,

$$\phi_{\mathbf{q}}(\tau) = \Delta \delta_{\mathbf{q}, \mathbf{0}} + \hat{\phi}_{\mathbf{q}}(\tau). \quad (48)$$

The effective action can be evaluated in powers of the fluctuation $\hat{\phi}_{\mathbf{q}}(\tau)$, i.e., $\mathcal{S}_{\text{eff}}^d = \mathcal{S}_0^d + \mathcal{S}_2^d + \dots$. The leading-order term \mathcal{S}_0^d represents the mean-field contribution. The Gaussian term \mathcal{S}_2^d represents the collective modes.

1. Mean-field approximation

The mean-field effective potential can be obtained in a way parallel to the p -wave pairing case. We obtain

$$\begin{aligned} \mathcal{S}_0^d(\Delta) &= \beta S \left[\frac{\Delta^2}{\lambda} + \int \frac{d^2\mathbf{k}}{(2\pi)^2} \xi_{\mathbf{k}} - \frac{T}{2} \sum_n \int \frac{d^2\mathbf{k}}{(2\pi)^2} \ln \text{Det} \mathcal{G}_{\mathbf{k}}^{-1}(i\omega_n) \right] \\ &= \beta S \left\{ \frac{\Delta^2}{\lambda} - \int \frac{d^2\mathbf{k}}{(2\pi)^2} \left[E_{\mathbf{k}} - \xi_{\mathbf{k}} + \sum_{s=\pm} T \ln \left(1 + e^{-\frac{E_{\mathbf{k}} + s\delta\mu}{T}} \right) \right] \right\}, \end{aligned} \quad (49)$$

where the dispersion is $E_{\mathbf{k}} = (\xi_{\mathbf{k}}^2 + |\Delta_{\mathbf{k}}^d|^2)^{1/2}$ with the gap function $\Delta_{\mathbf{k}}^d = \Delta \Gamma^d(\mathbf{k})$. The inverse fermion propagator reads

$$\mathcal{G}_{\mathbf{k}}^{-1}(i\omega_m) = \begin{pmatrix} (i\omega_m + \xi_{\mathbf{k}\uparrow}) & -\Delta_{\mathbf{k}}^d \\ -\Delta_{\mathbf{k}}^{d*} & (i\omega_m - \xi_{\mathbf{k}\downarrow}) \end{pmatrix}. \quad (50)$$

The saddle-point condition $\partial \mathcal{S}_0^d(\Delta) / \partial \Delta = 0$ gives the gap equation for the order parameter Δ ,

$$\frac{2}{\lambda} = \sum_{s=\pm} \int \frac{d^2\mathbf{k}}{(2\pi)^2} \frac{|\Gamma^d(\mathbf{k})|^2}{2E_{\mathbf{k}}} \tanh \left(\frac{E_{\mathbf{k}} + s\delta\mu}{2T} \right). \quad (51)$$

The number density can be obtained through the thermodynamic relation $n = -[\partial \mathcal{S}_{\text{eff}}^d(\Delta) / \partial \mu] / \beta S$. We obtain

$$n_0 \equiv \sum_{s=\pm} \int \frac{d^2\mathbf{k}}{(2\pi)^2} n_0(\mathbf{k}, s) = \frac{1}{2} \sum_{s=\pm} \int \frac{d^2\mathbf{k}}{(2\pi)^2} \left[1 - \frac{\xi_{\mathbf{k}}}{E_{\mathbf{k}}} \tanh \left(\frac{E_{\mathbf{k}} + s\delta\mu}{2T} \right) \right]. \quad (52)$$

Similar to the p -wave pairings, the interaction strength λ can be physically characterized by the two-body binding energy E_b in vacuum [19],

$$\frac{1}{\lambda} = \int \frac{d^2\mathbf{k}}{(2\pi)^2} \frac{|\Gamma^d(\mathbf{k})|^2}{2\epsilon_{\mathbf{k}} - E_b}. \quad (53)$$

The weak and strong attraction limits correspond to $E_b \rightarrow +\infty$ and $E_b \rightarrow -\infty$, respectively.

2. Gaussian fluctuation and Goldstone mode

Similar to the p -wave pairing case, the effective action for the collective modes can be evaluated as

$$\mathcal{S}_2^d = \sum_{\mathbf{q}, n} \left\{ \frac{|\hat{\phi}_{\mathbf{q}}(i\nu_n)|^2}{\lambda} + \frac{T}{2S} \sum_{\mathbf{k}, m} \text{tr}[\mathcal{G}_{\mathbf{k}-\mathbf{q}/2}(i\omega_m) \times \Phi_{-\mathbf{q}}(-i\nu_n) \mathcal{G}_{\mathbf{k}+\mathbf{q}/2}(i\omega_m + i\nu_n) \Phi_{\mathbf{q}}(i\nu_n)] \right\}, \quad (54)$$

where the fermion propagator and the matrix Φ are given by

$$\mathcal{G}_{\mathbf{k}}(i\omega_n) = \frac{1}{(i\omega_n - \delta\mu)^2 - E_{\mathbf{k}}^2} \begin{pmatrix} (i\omega_n - \xi_{\mathbf{k}\downarrow}) & \Delta_{\mathbf{k}}^d \\ \Delta_{\mathbf{k}}^{d*} & (i\omega_n + \xi_{\mathbf{k}\uparrow}) \end{pmatrix},$$

$$\Phi_{\mathbf{q}}(i\nu_n) = \begin{pmatrix} 0 & -\hat{\phi}_{\mathbf{q}}(i\nu_n)\Gamma^d(\mathbf{k}) \\ -\hat{\phi}_{-\mathbf{q}}^*(-i\nu_n)\Gamma^{d*}(\mathbf{k}) & 0 \end{pmatrix}. \quad (55)$$

After some algebra, \mathcal{S}_2^d can be written in a compact form,

$$\mathcal{S}_2^d = \frac{1}{2} \sum_{\mathbf{q}, n} \begin{pmatrix} \hat{\phi}_{\mathbf{q}}^*(i\nu_n) & \hat{\phi}_{-\mathbf{q}}(-i\nu_n) \end{pmatrix} M(\mathbf{q}, i\nu_n) \begin{pmatrix} \hat{\phi}_{\mathbf{q}}(i\nu_n) \\ \hat{\phi}_{-\mathbf{q}}^*(-i\nu_n) \end{pmatrix}, \quad (56)$$

where the inverse boson propagator $M(\mathbf{q}, i\nu_n)$ takes the form

$$M(\mathbf{q}, i\nu_n) = \begin{pmatrix} M_{11}(\mathbf{q}, i\nu_n) & M_{12}(\mathbf{q}, i\nu_n) \\ M_{21}(\mathbf{q}, i\nu_n) & M_{22}(\mathbf{q}, i\nu_n) \end{pmatrix}. \quad (57)$$

The matrix elements of M are given by

$$M_{11} = \frac{1}{\lambda} + \frac{T}{S} \sum_{\mathbf{k}, m} \mathcal{G}_{\mathbf{k}-\mathbf{q}/2}^{11}(i\omega_m) \mathcal{G}_{\mathbf{k}+\mathbf{q}/2}^{22}(i\omega_m + i\nu_n) |\Gamma^d(\mathbf{k})|^2,$$

$$M_{22} = \frac{1}{\lambda} + \frac{T}{S} \sum_{\mathbf{k}, m} \mathcal{G}_{\mathbf{k}-\mathbf{q}/2}^{22}(i\omega_m) \mathcal{G}_{\mathbf{k}+\mathbf{q}/2}^{11}(i\omega_m + i\nu_n) |\Gamma^d(\mathbf{k})|^2,$$

$$M_{12} = \frac{T}{S} \sum_{\mathbf{k}, m} \mathcal{G}_{\mathbf{k}-\mathbf{q}/2}^{12}(i\omega_m) \mathcal{G}_{\mathbf{k}+\mathbf{q}/2}^{12}(i\omega_m + i\nu_n) [\Gamma^{d*}(\mathbf{k})]^2,$$

$$M_{21} = \frac{T}{S} \sum_{\mathbf{k}, m} \mathcal{G}_{\mathbf{k}-\mathbf{q}/2}^{21}(i\omega_m) \mathcal{G}_{\mathbf{k}+\mathbf{q}/2}^{21}(i\omega_m + i\nu_n) [\Gamma^d(\mathbf{k})]^2. \quad (58)$$

It is easy to prove that these matrix elements satisfy

$$M_{11}^*(\mathbf{q}, i\nu_n) = M_{22}(\mathbf{q}, i\nu_n), \quad M_{12}^*(\mathbf{q}, i\nu_n) = M_{21}(\mathbf{q}, i\nu_n). \quad (59)$$

Completing the summation over the fermion Matsubara frequency $i\omega_m$, we obtain

$$M_{11} = \frac{1}{\lambda} + \sum_{s=\pm} \int \frac{d^2\mathbf{k}}{(2\pi)^2} \frac{|\Gamma^d(\mathbf{k})|^2}{2} \left[\left(\frac{u_+^2 v_+^2}{i\nu_n + (E_+ - E_-)} - \frac{u_+^2 v_-^2}{i\nu_n - (E_+ - E_-)} \right) (f_+^s - f_-^s) \right. \\ \left. + \left(\frac{u_+^2 u_-^2}{i\nu_n - (E_+ + E_-)} - \frac{v_+^2 v_-^2}{i\nu_n + (E_+ + E_-)} \right) (1 - f_+^s - f_-^s) \right],$$

$$M_{12} = - \sum_{s=\pm} \int \frac{d^2\mathbf{k}}{(2\pi)^2} \frac{[\Gamma^{d*}(\mathbf{k})]^2}{8E_+ E_-} \left[\left(\frac{\Delta_{\mathbf{k}-\mathbf{q}/2}^d \Delta_{\mathbf{k}+\mathbf{q}/2}^d}{i\nu_n - (E_+ - E_-)} - \frac{\Delta_{\mathbf{k}-\mathbf{q}/2}^d \Delta_{\mathbf{k}+\mathbf{q}/2}^d}{i\nu_n + (E_+ - E_-)} \right) (f_+^s - f_-^s) \right. \\ \left. + \left(\frac{\Delta_{\mathbf{k}-\mathbf{q}/2}^d \Delta_{\mathbf{k}+\mathbf{q}/2}^d}{i\nu_n - (E_+ + E_-)} - \frac{\Delta_{\mathbf{k}-\mathbf{q}/2}^d \Delta_{\mathbf{k}+\mathbf{q}/2}^d}{i\nu_n + (E_+ + E_-)} \right) (1 - f_+^s - f_-^s) \right], \quad (60)$$

where the Fermi-Dirac distribution function is given by $f_{\pm}^s = (1 + e^{(E_{\pm} + s\delta\mu)/T})^{-1}$. Again, we note that the terms proportional to $f_+^s - f_-^s$ correspond to the Landau damping effect, which vanish for the balanced case $\delta\mu = 0$ when $T \rightarrow 0$.

It is more physical to decompose the collective mode $\hat{\phi}(x)$ into a sum of real and imaginary parts, that is, $\hat{\phi}(x) = \sigma(x) + i\pi(x)$. Then the Gaussian fluctuation part of the effective action can be reexpressed as

$$\mathcal{S}_2^d = \frac{1}{2} \sum_{\mathbf{q}, n} [\sigma_{\mathbf{q}}^*(i\nu_n) \quad \pi_{\mathbf{q}}^*(i\nu_n)] \Pi(\mathbf{q}, i\nu_n) \begin{pmatrix} \sigma_{\mathbf{q}}(i\nu_n) \\ \pi_{\mathbf{q}}(i\nu_n) \end{pmatrix}, \quad (61)$$

where the effective inverse boson propagator is

$$\Pi = \begin{pmatrix} (M_{11} + M_{12} + M_{21} + M_{22}) & i(-M_{11} - M_{12} + M_{21} + M_{22}) \\ i(M_{11} - M_{12} + M_{21} - M_{22}) & (M_{11} - M_{12} - M_{21} + M_{22}) \end{pmatrix}. \quad (62)$$

Thus, all the matrix elements of Π are real and the propagators of independent collective modes can be obtained through the diagonalization, and we find

$$\mathcal{D}_{\theta/\eta}^{-1}(\mathbf{q}, i\nu_n) = M_{11} + M_{22} \mp \sqrt{(M_{11} - M_{22})^2 + 4M_{12}M_{21}}. \quad (63)$$

It can be verified that $\mathcal{D}_{\theta}^{-1}(0,0) = 0$, which shows θ to be the Goldstone mode with the following mixing of σ and π components:

$$\theta_{\mathbf{q}}(i\nu_n) = C[\mathcal{D}_{\theta}^{-1}(\mathbf{q}, i\nu_n)\sigma_{\mathbf{q}}(i\nu_n) + \mathcal{D}_{\eta}^{-1}(\mathbf{q}, i\nu_n)\pi_{\mathbf{q}}(i\nu_n)], \quad (64)$$

where C is a normalization coefficient.

The approach for the KT and VAL transitions is the same as we adopted for the p -wave pairing. At small energy and momentum, the propagator of the gapless θ mode can be expressed as

$$\mathcal{D}_{\theta}^{-1}(\mathbf{q}, i\nu_n) = -\zeta^d(i\nu_n)^2 + \frac{1}{4m\Delta^2}\rho^d\mathbf{q}^2, \quad (65)$$

where we can show that the stiffness ρ^d is isotropic for both isotropic and anisotropic d -wave pairings. To compute the coefficients ζ^d and ρ^d , we make the low-energy expansion of M_{ij} ($i, j = 1, 2$) to the quadratic order in frequency and momentum,

$$M_{ij}(\mathbf{q}, i\nu_n) = A_{ij} + i\nu_n B_{ij} + (i\nu_n)^2 C_{ij} + D_{ij}^x q_x^2 + D_{ij}^y q_y^2. \quad (66)$$

The Landau damping problem still exists here. We again neglect the damping of collective modes and perform this expansion. The expansion coefficients read

$$\begin{aligned} A_{11} = A_{22} &= \frac{1}{\lambda} - \frac{1}{S} \sum_{\mathbf{k}, s=\pm} (E_{\mathbf{k}}^2 + \xi_{\mathbf{k}}^2) \frac{|\Gamma^d(\mathbf{k})|^2}{8E_{\mathbf{k}}^3} \\ &\times \tanh\left(\frac{E_{\mathbf{k}} + s\delta\mu}{2T}\right), \\ B_{11} = -B_{22} &= -\frac{1}{S} \sum_{\mathbf{k}, s=\pm} \frac{\xi_{\mathbf{k}}|\Gamma^d(\mathbf{k})|^2}{8E_{\mathbf{k}}^3} \tanh\left(\frac{E_{\mathbf{k}} + s\delta\mu}{2T}\right), \\ C_{11} = C_{22} &= -\frac{1}{S} \sum_{\mathbf{k}, s=\pm} (E_{\mathbf{k}}^2 + \xi_{\mathbf{k}}^2) \frac{|\Gamma^d(\mathbf{k})|^2}{32E_{\mathbf{k}}^5} \\ &\times \tanh\left(\frac{E_{\mathbf{k}} + s\delta\mu}{2T}\right), \\ A_{12} = A_{21} &= \frac{1}{S} \sum_{\mathbf{k}, s=\pm} \frac{|\Delta_{\mathbf{k}}^d|^2 |\Gamma^d(\mathbf{k})|^2}{8E_{\mathbf{k}}^3} \tanh\left(\frac{E_{\mathbf{k}} + s\delta\mu}{2T}\right), \\ B_{12} = B_{21} &= 0, \\ C_{12} = C_{21} &= \frac{1}{S} \sum_{\mathbf{k}, s=\pm} \frac{|\Delta_{\mathbf{k}}^d|^2 |\Gamma^d(\mathbf{k})|^2}{32E_{\mathbf{k}}^5} \tanh\left(\frac{E_{\mathbf{k}} + s\delta\mu}{2T}\right). \end{aligned} \quad (67)$$

The coefficients D_{ij} are again rather lengthy and we show the combined quantities,

$$\rho_i^d = 4m\Delta^2(D_{11}^i + D_{22}^i - D_{12}^i - D_{21}^i), \quad i = x, y, \quad (68)$$

which are exactly the superfluid densities along the x and y directions. After a lengthy calculation, we obtain

$$\rho_i^d = \sum_{s=\pm} \int \frac{d^2\mathbf{k}}{(2\pi)^2} \left[n_0(\mathbf{k}, s) - \frac{k_i^2}{4mT} \operatorname{sech}^2\left(\frac{E_{\mathbf{k}} + s\delta\mu}{2T}\right) \right]. \quad (69)$$

Compared to p -wave pairing, the superfluid density is isotropic for both $d_{x^2-y^2} + 2id_{xy}$ and $d_{x^2-y^2}$ pairings at any temperature. We have $\rho_x^d = \rho_y^d = \rho^d$.

Finally, the low-energy behavior of the θ mode or the Goldstone mode can be given by Eq. (65), where $\zeta^d = \zeta_0^d + B_{11}^2/A_{12}$ with $\zeta_0^d = -2(C_{11} - C_{12})$. The sound velocity is given by

$$v^d = \sqrt{\frac{\rho^d}{4m\Delta^2\zeta^d}}. \quad (70)$$

As mentioned in the p -wave case, the coupling term B_{11}^2/A_{12} ensures that we recover the correct sound velocity in the BCS-BEC evolution. The Goldstone-mode contribution to the thermodynamic potential can be given by

$$\Omega_2^d = \int \frac{d^2\mathbf{q}}{(2\pi)^2} T \ln(1 - e^{-\varepsilon_{\mathbf{q}}/T}) = -\frac{\zeta(3)T^3}{2\pi(v^d)^2}, \quad (71)$$

where the dispersion relation is $\varepsilon_{\mathbf{q}} = v^d|\mathbf{q}|$. At finite temperature, we take into account the fluctuation contribution to the number density. The total fermion density n is given by

$$n = n_0 - \frac{\partial\Omega_2^d}{\partial\mu} = n_0 - \frac{\zeta(3)T^3}{\pi(v^d)^3} \frac{\partial v^d}{\partial\mu}, \quad (72)$$

which reduces to the mean-field result $n = n_0$ at zero temperature.

B. KT and VAL melting transitions

In the following, we explore the feature of KT and VAL transitions in this spin-1/2 Fermi system with d -wave pairing. The KT and VAL melting temperatures are both directly related to the stiffness $J = \rho^d/(4m)$ in the following way [35–37, 53]:

$$T_{\text{KT}} = \frac{\pi}{2} J^d(T_{\text{KT}}), \quad T_{\text{M}} = 0.3J^d(T_{\text{M}}). \quad (73)$$

The transition temperatures T_{KT} and T_{M} can be determined by self-consistently solving the gap equation (51), the number equation (72), and critical temperature equation (73). In the following, we will consider balanced ($\delta\mu = 0$) and imbalanced ($\delta\mu \neq 0$) systems. To present the numerical results, we define the Fermi momentum k_{F} and Fermi energy ε_{F} of a noninteracting balanced Fermi gas, through $n = k_{\text{F}}^2/(2\pi)$ and $\varepsilon_{\text{F}} = k_{\text{F}}^2/(2m)$.

1. Balanced Fermi gases

For the balanced system with $\delta\mu = 0$, the numerical results are shown in Fig. 3. The transition temperatures T_{KT} and T_{M} approach constants in the deep BEC region, $T_{\text{KT}} = 0.125\varepsilon_{\text{F}}$ and $T_{\text{M}} = (0.6/\pi)T_{\text{KT}}$, as we found in the p -wave pairing case.

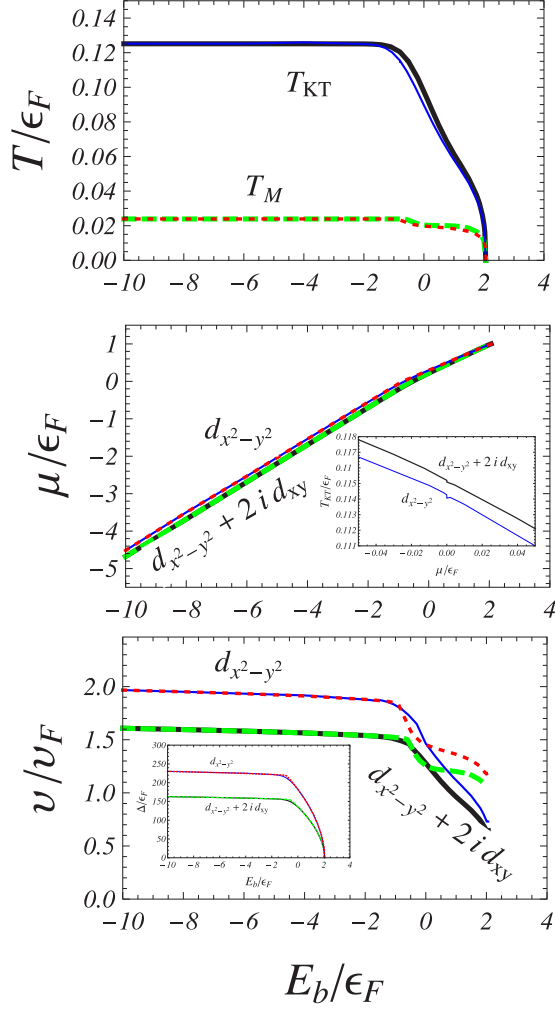


FIG. 3. Upper panel: The transition temperatures, T_{KT} (solid lines) and T_M (dashed lines), as functions of the two-body binding energy E_b for the isotropic $d_{x^2-y^2} + 2id_{xy}$ pairing (black and green thick lines) and the anisotropic $d_{x^2-y^2}$ pairing (blue and red thin lines). Lower panels: The chemical potential μ and sound velocity v as functions of E_b at T_{KT} and T_M . The insets show the zoom-in plots of T_{KT} with respect to μ around the BCS-BEC transition point $\mu = 0$ and the order parameter Δ as a function of E_b . The parameters for the NSR potential are $k_0 = 10^{3/2}k_F$ and $k_1 = 10^{1/2}k_F$.

The chemical potential, the order parameter, and the sound velocity are not sensitive to the temperature. At intermediate and at strong coupling, their values at T_M and T_{KT} are almost the same.

For the d -wave pairing case, the nonanalyticity is also found at the BCS-BEC transition point $\mu = 0$. To see this, we can take the same argument as we gave for the p -wave pairing case. We explore the properties of the most relevant quantity ζ_0^d around $\mu = 0$. The derivative of ζ_0^d with respect to μ is given by

$$\frac{\partial \zeta_0^d}{\partial \mu} = \int \frac{d^2 \mathbf{k}}{(2\pi)^2} \frac{\xi_{\mathbf{k}} |\Gamma^d(\mathbf{k})|^2}{4E_{\mathbf{k}}^4} \left[\frac{3 \tanh\left(\frac{E_{\mathbf{k}}}{2T}\right)}{E_{\mathbf{k}}} - \frac{\text{sech}^2\left(\frac{E_{\mathbf{k}}}{2T}\right)}{2T} \right], \quad (74)$$

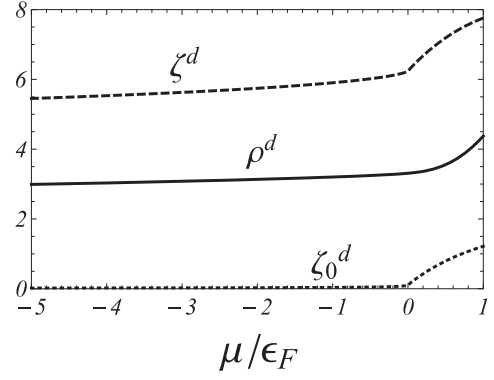


FIG. 4. The behavior of the quantities ζ_0^d , ζ^d , and ρ^d with respect to the chemical potential μ for the $d_{x^2-y^2} + 2id_{xy}$ pairing. These quantities have been scaled by proper constants so that they are dimensionless in the plot and the magnitudes are all increased by multiplying 10^6 . In the calculations, we choose $T = 0.12\epsilon_F$ and $\Delta = 150\epsilon_F$. The parameters for the NSR potential are the same as used in Fig. 3.

which is divergent logarithmically at $\mu = 0$. This further induces nonanalyticities in n , T_{KT} , T_M , etc. In the numerical results shown in Fig. 3, the nonanalyticities are not obvious for the present choice of the parameters k_0 and k_1 ; however, we can easily identify the nonanalyticity in the inset figure for T_{KT} .

Unlike the p -wave pairing case, the sound velocity for d -wave pairing does not show nonmonotonicity: it is always a decreasing function when E_b goes from negative to positive. This can be understood from Fig. 4: As ζ^d always increases faster than ρ^d with μ , the sound velocity v^d decreases monotonously with the binding energy E_b .

2. Mismatched Fermi gases

In order to study the effect of mismatched Fermi surfaces ($\delta\mu \neq 0$) on KT and VAL melting transitions, we choose a fixed binding energy $E_b = -2\epsilon_F$ which lies in the BEC region as an example.

We plot the transition temperatures T_{KT} and T_M , the chemical potentials at T_{KT} and T_M , the order parameters Δ at T_{KT} and T_M , and the sound velocity v at T_{KT} and T_M as functions of $\delta\mu$ in Fig. 5. As we expect, all of these quantities decrease with $\delta\mu$. For small $\delta\mu$, the decreasing effect is not significant. However, for large $\delta\mu$, they almost linearly decrease with $\delta\mu$ and finally reach a critical point $\delta\mu_c \sim 3\epsilon_F$ beyond which the superfluidity is destroyed, and the KT and VAL melting transition temperatures both approach zero at this point.

IV. SUMMARY

In this work, the features of the Kosterlitz-Thouless and vortex-antivortex lattice melting transitions are explored in detail for fermionic systems with higher partial wave pairings, including p -wave and d -wave pairings. The KT and VAL melting transitions are obtained by studying the low-energy dynamics of the gapless Goldstone mode. Our approach takes into account both the amplitude and phase modes and can recover the correct sound velocity in the BCS-BEC evolution,

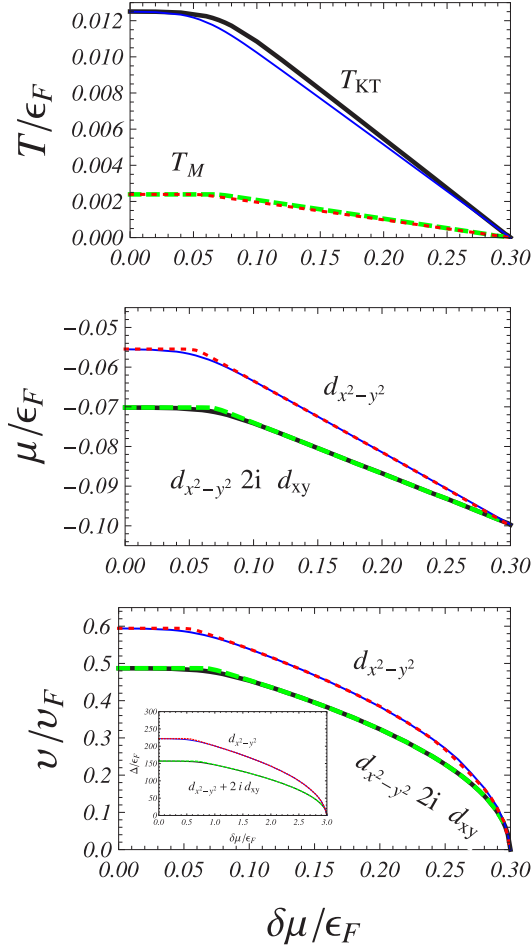


FIG. 5. Upper panel: The transition temperatures, T_{KT} (solid lines) and T_M (dashed lines), as functions of the Zeeman field $\delta\mu$ with a fixed binding energy $E_b = -2\epsilon_F$ for the isotropic $d_{x^2-y^2} + 2i d_{xy}$ pairing (black and green thick lines) and the anisotropic $d_{x^2-y^2}$ pairing (blue and red thin lines). Lower panels: The chemical potential μ and sound velocity v as functions of $\delta\mu$ at T_{KT} and T_M . The inset shows the order parameter Δ as a function of $\delta\mu$. The parameters for the NSR potential are the same as used in Fig. 3.

which enables us to include correctly the collective modes contribution to the thermodynamics.

The main results of this work can be summarized as follows:

(a) For the p -wave pairing, we find that the transition temperatures T_{KT} and T_M approach constants in the BEC region: $T_{KT} = 0.0625\epsilon_F$ and $T_M = (0.6/\pi)T_{KT}$. The KT transition temperature is thus reachable in current cold-atom experiments. The transition temperatures and the sound velocities are continuous but nonanalytic across the BCS-BEC transition point $\mu = 0$. For the anisotropic p_x pairing, the sound velocity is anisotropic in the BCS region, but becomes nearly isotropic in the BEC region. The sound velocity exhibits nonmonotonic behavior and may be used to probe the BCS-BEC transition in Fermi gases with p -wave pairing.

(b) For d -wave pairing, the transition temperatures T_{KT} and T_M also approach constants in the BEC region: $T_{KT} = 0.125\epsilon_F$ and $T_M = (0.6/\pi)T_{KT}$. The transition temperatures and sound velocities are noncontinuous across the BCS-BEC transition point $\mu = 0$ because of the higher divergence degree [25]. Because of the exchange symmetry between k_x and k_y , the sound velocity is isotropic even for the anisotropic $d_{x^2-y^2}$ pairing. We find that the effect of mismatched Fermi surfaces also destroys the d -wave superfluidity and the associated KT transition.

ACKNOWLEDGMENTS

We thank Hui Hu for the discussion. This work is supported by the Thousand Young Talents Program of China. G.C. and X.G.H. are also supported by the NSFC with Grants No. 11535012 and No. 11675041, and the Scientific Research Foundation of State Education Ministry for Returned Scholars. G.C. is also supported by the China Postdoctoral Science Foundation with Grant No. KLH1512072. L.H. acknowledges the support by the NSFC with Grant No. 11775123.

APPENDIX: THE EXPANSION COEFFICIENTS FOR THE θ MODE

In order to obtain the analytic form of the stiffness, we expand $M_{11} + M_{22} - M_{12} - M_{21}$ for small \mathbf{q} at $i\nu_n = 0$. We take the d -wave pairing case as an example and the p -wave pairing case is similar. The relevant term is

$$F(\mathbf{q}) = \sum_{\mathbf{k}, m} \frac{1}{[(i\tilde{\omega}_m)^2 - E_{\mathbf{k}-\mathbf{q}/2}^2][(i\tilde{\omega}_m)^2 - E_{\mathbf{k}+\mathbf{q}/2}^2]} \{2(i\tilde{\omega}_m - \xi_{\mathbf{k}-\mathbf{q}/2})(i\tilde{\omega}_m + \xi_{\mathbf{k}+\mathbf{q}/2})|\Gamma^d(\mathbf{k})|^2 - \Delta_{\mathbf{k}-\mathbf{q}/2}\Delta_{\mathbf{k}+\mathbf{q}/2}[\Gamma^{d*}(\mathbf{k})]^2 - \Delta_{\mathbf{k}-\mathbf{q}/2}^*\Delta_{\mathbf{k}+\mathbf{q}/2}^*[\Gamma^d(\mathbf{k})]^2\}, \quad (\text{A1})$$

where $i\tilde{\omega}_m = i\omega_m - \delta\mu$. The first derivative of $F(\mathbf{q})$ with respect to q_i ($i = x, y$) is

$$\partial_{q_i} F(\mathbf{q}) = \sum_{\mathbf{k}, m} \frac{1}{[(i\tilde{\omega}_m)^2 - E_{\mathbf{k}-\mathbf{q}/2}^2][(i\tilde{\omega}_m)^2 - E_{\mathbf{k}+\mathbf{q}/2}^2]} \left\{ [\partial_{k_i} \xi_{\mathbf{k}-\mathbf{q}/2}(i\tilde{\omega}_m + \xi_{\mathbf{k}+\mathbf{q}/2}) + \partial_{k_i} \xi_{\mathbf{k}+\mathbf{q}/2}(i\tilde{\omega}_m - \xi_{\mathbf{k}-\mathbf{q}/2})] |\Gamma^d(\mathbf{k})|^2 + \frac{1}{2}(\Delta'_{\mathbf{k}-\mathbf{q}/2}\Delta_{\mathbf{k}+\mathbf{q}/2} - \Delta_{\mathbf{k}-\mathbf{q}/2}\Delta'_{\mathbf{k}+\mathbf{q}/2})[\Gamma^{d*}(\mathbf{k})]^2 + \frac{1}{2}(\Delta_{\mathbf{k}-\mathbf{q}/2}^*\Delta'_{\mathbf{k}+\mathbf{q}/2} - \Delta_{\mathbf{k}-\mathbf{q}/2}^*\Delta_{\mathbf{k}+\mathbf{q}/2}^*)[\Gamma^d(\mathbf{k})]^2 \right\}$$

$$\begin{aligned}
& - \sum_{\mathbf{k}, m} \frac{1}{2[(i\tilde{\omega}_m)^2 - E_{\mathbf{k}-\mathbf{q}/2}^2]^2 [(i\tilde{\omega}_m)^2 - E_{\mathbf{k}+\mathbf{q}/2}^2]^2} \left\{ (E_{\mathbf{k}-\mathbf{q}/2}^2)' [(i\tilde{\omega}_m)^2 - E_{\mathbf{k}+\mathbf{q}/2}^2] - (E_{\mathbf{k}+\mathbf{q}/2}^2)' [(i\tilde{\omega}_m)^2 - E_{\mathbf{k}-\mathbf{q}/2}^2] \right\} \\
& \times \{ 2(i\tilde{\omega}_m - \xi_{\mathbf{k}-\mathbf{q}/2})(i\tilde{\omega}_m + \xi_{\mathbf{k}+\mathbf{q}/2}) |\Gamma^d(\mathbf{k})|^2 - \Delta_{\mathbf{k}-\mathbf{q}/2} \Delta_{\mathbf{k}+\mathbf{q}/2} [\Gamma^{d*}(\mathbf{k})]^2 - \Delta_{\mathbf{k}-\mathbf{q}/2}^* \Delta_{\mathbf{k}+\mathbf{q}/2}^* [\Gamma^d(\mathbf{k})]^2 \}. \quad (\text{A2})
\end{aligned}$$

Here we use the notation $A' = \partial_{q_i} A$. Keeping in mind that $[(i\tilde{\omega}_m)^2 - E_{\mathbf{k}-\mathbf{q}/2}^2][(i\tilde{\omega}_m)^2 - E_{\mathbf{k}+\mathbf{q}/2}^2]$ is an even function of \mathbf{q} , we can evaluate the second derivative of $F(\mathbf{q})$ around $\mathbf{q} = 0$ as

$$\begin{aligned}
\partial_{q_i}^2 F(\mathbf{q})|_{\mathbf{q}=0} &= \sum_{\mathbf{k}, m} \frac{1}{[(i\tilde{\omega}_m)^2 - E_{\mathbf{k}}^2]^2} \left\{ [\xi_{\mathbf{k}} \partial_{k_i}^2 \xi_{\mathbf{k}} + 3(\partial_{k_i} \xi_{\mathbf{k}})^2] |\Gamma^d(\mathbf{k})|^2 + \frac{\Delta^2}{4} (|\Gamma^d(\mathbf{k})|^4)'' \right\} \\
&+ \sum_{\mathbf{k}, m} \frac{4|\Gamma^d(\mathbf{k})|^2}{[(i\tilde{\omega}_m)^2 - E_{\mathbf{k}}^2]^3} \left[\xi_{\mathbf{k}} \partial_{k_i} \xi_{\mathbf{k}} + \frac{1}{2} (|\Delta_{\mathbf{k}}|^2)' \right]^2. \quad (\text{A3})
\end{aligned}$$

Finally, we complete the Matsubara frequency summation and obtain

$$\begin{aligned}
\partial_{q_i}^2 F(\mathbf{q})|_{\mathbf{q}=0} &= \sum_{\mathbf{k}, s=\pm} \left\{ [\xi_{\mathbf{k}} \partial_{k_i}^2 \xi_{\mathbf{k}} + 3(\partial_{k_i} \xi_{\mathbf{k}})^2] |\Gamma^d(\mathbf{k})|^2 + \frac{\Delta^2}{4} (|\Gamma^d(\mathbf{k})|^4)'' \right\} \left[\frac{\tanh\left(\frac{E_{\mathbf{k}}^s}{2T}\right)}{8E_{\mathbf{k}}^3} - \frac{\text{sech}^2\left(\frac{E_{\mathbf{k}}^s}{2T}\right)}{16TE_{\mathbf{k}}^2} \right] \\
&+ \sum_{\mathbf{k}, s=\pm} \left[\xi_{\mathbf{k}} \partial_{k_i} \xi_{\mathbf{k}} + \frac{1}{2} (|\Delta_{\mathbf{k}}|^2)' \right]^2 \frac{|\Gamma^d(\mathbf{k})|^2}{8E_{\mathbf{k}}^3} \left[-\frac{3 \tanh\left(\frac{E_{\mathbf{k}}^s}{2T}\right)}{E_{\mathbf{k}}^2} + \frac{3 \text{sech}^2\left(\frac{E_{\mathbf{k}}^s}{2T}\right)}{2TE_{\mathbf{k}}} + \frac{\tanh\left(\frac{E_{\mathbf{k}}^s}{2T}\right) \text{sech}^2\left(\frac{E_{\mathbf{k}}^s}{2T}\right)}{2T^2} \right]. \quad (\text{A4})
\end{aligned}$$

Here, $E_{\mathbf{k}}^s = E_{\mathbf{k}} + s\delta\mu$ for convenience.

For s -wave or p -wave pairing, we only need to change the corresponding γ functions $\Gamma^d(\mathbf{k})$ to $\Gamma^{s,p}(\mathbf{k})$ and set $\delta\mu \equiv 0$ for the p -wave case. For s -wave pairing where $\Gamma^s(\mathbf{k}) = 1$, Eq. (A3) becomes

$$\partial_{q_i}^2 F(\mathbf{q})|_{\mathbf{q}=0} = \sum_{\mathbf{k}, m} \left\{ \frac{\xi_{\mathbf{k}} \partial_{k_i}^2 \xi_{\mathbf{k}} + 3(\partial_{k_i} \xi_{\mathbf{k}})^2}{[(i\tilde{\omega}_m)^2 - E_{\mathbf{k}}^2]^2} + \frac{4(\xi_{\mathbf{k}} \partial_{k_i} \xi_{\mathbf{k}})^2}{[(i\tilde{\omega}_m)^2 - E_{\mathbf{k}}^2]^3} \right\}. \quad (\text{A5})$$

Using the following identities:

$$\begin{aligned}
& -\frac{\partial}{\partial \mu} \frac{\xi_{\mathbf{k}}}{[(i\tilde{\omega}_m)^2 - E_{\mathbf{k}}^2]^2} = \frac{1}{[(i\tilde{\omega}_m)^2 - E_{\mathbf{k}}^2]^2} + \frac{4\xi_{\mathbf{k}}^2}{[(i\tilde{\omega}_m)^2 - E_{\mathbf{k}}^2]^3}, \quad (\text{A6}) \\
& -\sum_{\mathbf{k}, m} (\partial_{k_i} \xi_{\mathbf{k}})^2 \frac{\partial}{\partial \mu} \frac{\xi_{\mathbf{k}}}{[(i\tilde{\omega}_m)^2 - E_{\mathbf{k}}^2]^2} = \sum_{\mathbf{k}, m} (\partial_{k_i} \xi_{\mathbf{k}})^2 \frac{\partial}{\partial \xi_{\mathbf{k}}} \frac{\xi_{\mathbf{k}}}{[(i\tilde{\omega}_m)^2 - E_{\mathbf{k}}^2]^2} = \frac{2m}{4\pi} \sum_m \int_0^\infty d\xi_{\mathbf{k}} (\partial_{k_i} \xi_{\mathbf{k}})^2 \frac{\partial}{\partial \xi_{\mathbf{k}}} \frac{\xi_{\mathbf{k}}}{[(i\tilde{\omega}_m)^2 - E_{\mathbf{k}}^2]^2} \\
& = -\frac{2m}{4\pi} \sum_m \int_0^\infty d\xi_{\mathbf{k}} \partial_{k_i}^2 \xi_{\mathbf{k}} \frac{\xi_{\mathbf{k}}}{[(i\tilde{\omega}_m)^2 - E_{\mathbf{k}}^2]^2} = -\sum_{\mathbf{k}, m} \partial_{k_i}^2 \xi_{\mathbf{k}} \frac{\xi_{\mathbf{k}}}{[(i\tilde{\omega}_m)^2 - E_{\mathbf{k}}^2]^2}, \quad (\text{A7})
\end{aligned}$$

we obtain

$$\partial_{q_i}^2 F(\mathbf{q})|_{\mathbf{q}=0} = \sum_{\mathbf{k}, m} \frac{2(\partial_{k_i} \xi_{\mathbf{k}})^2}{[(i\tilde{\omega}_m)^2 - E_{\mathbf{k}}^2]^2} = \sum_{\mathbf{k}} \frac{\mathbf{k}^2}{4m^2 E_{\mathbf{k}}^2} \left[\frac{\tanh\left(\frac{E_{\mathbf{k}}}{2T}\right)}{E_{\mathbf{k}}} - \frac{\text{sech}^2\left(\frac{E_{\mathbf{k}}}{2T}\right)}{2T} \right] \quad (\text{A8})$$

at $\delta\mu = 0$. This is equivalent to the explicit form given in [53].

-
- [1] D. M. Eagles, *Phys. Rev.* **186**, 456 (1969).
[2] A. J. Leggett, in *Modern Trends in the Theory of Condensed Matter*, edited by A. Pekalski and J. Przystawa (Springer-Verlag, Berlin, 1980).
[3] P. Nozieres and S. Schmitt-Rink, *J. Low Temp. Phys.* **59**, 195 (1985).
[4] C. A. R. Sa de Melo, M. Randeria, and J. R. Engelbrecht, *Phys. Rev. Lett.* **71**, 3202 (1993).
[5] J. R. Engelbrecht, M. Randeria, and C. A. R. Sa de Melo, *Phys. Rev. B* **55**, 15153 (1997).
[6] M. Randeria, J.-M. Duan, and L.-Y. Shieh, *Phys. Rev. Lett.* **62**, 981 (1989).
[7] M. Randeria, J.-M. Duan, and L.-Y. Shieh, *Phys. Rev. B* **41**, 327 (1990).
[8] V. M. Loktev, R. M. Quick, and S. G. Sharapov, *Phys. Rep.* **349**, 1 (2001).
[9] Q. Chen, J. Stajic, S. Tan, and K. Levin, *Phys. Rep.* **412**, 1 (2005).
[10] S. Giorgini, L. P. Pitaevskii, and S. Stringari, *Rev. Mod. Phys.* **80**, 1215 (2008).

- [11] V. Gurarie and L. Radzihovsky, *Ann. Phys. (NY)* **322**, 2 (2007).
- [12] M. Greiner, C. A. Regal, and D. S. Jin, *Nature (London)* **426**, 537 (2003).
- [13] S. Jochim, M. Bartenstein, A. Altmeyer, G. Hendl, S. Riedl, C. Chin, J. Hecker Denschlag, and R. Grimm, *Science* **302**, 2101 (2003).
- [14] M. W. Zwierlein, J. R. Abo-Shaeer, A. Schirotzek, C. H. Schunck, and W. Ketterle, *Nature (London)* **435**, 1047 (2003).
- [15] R. Combescot, M. Yu. Kagan, and S. Stringari, *Phys. Rev. A* **74**, 042717 (2006).
- [16] L. Belkhir and M. Randeria, *Phys. Rev. B* **45**, 5087 (1992).
- [17] L. Belkhir and M. Randeria, *Phys. Rev. B* **49**, 6829 (1994).
- [18] N. Read and D. Green, *Phys. Rev. B* **61**, 10267 (2000).
- [19] S. S. Botelho and C. A. R. Sá de Melo, *J. Low Temp. Phys.* **140**, 409 (2005).
- [20] S. S. Botelho and C. A. R. Sá de Melo, *Phys. Rev. B* **71**, 134507 (2005).
- [21] V. Gurarie, L. Radzihovsky, and A. V. Andreev, *Phys. Rev. Lett.* **94**, 230403 (2005).
- [22] C.-H. Cheng and S.-K. Yip, *Phys. Rev. Lett.* **95**, 070404 (2005).
- [23] M. Iskin and C. A. R. Sa de Melo, *Phys. Rev. Lett.* **96**, 040402 (2006).
- [24] M. Iskin and C. A. R. Sa de Melo, *Phys. Rev. A* **74**, 013608 (2006).
- [25] G. Cao, L. He, and P. Zhuang, *Phys. Rev. A* **87**, 013613 (2013).
- [26] C. Luciuk, S. Trotzky, S. Smale, Z. Yu, S. Zhang, and J. H. Thywissen, *Nat. Phys.* **12**, 599 (2016).
- [27] S. Dong, Y. Cui, C. Shen, Y. Wu, M. K. Tey, L. You, and B. Gao, *Phys. Rev. A* **94**, 062702 (2016).
- [28] S. M. Yoshida and M. Ueda, *Phys. Rev. Lett.* **115**, 135303 (2015).
- [29] Z. Yu, J. H. Thywissen, and S. Zhang, *Phys. Rev. Lett.* **115**, 135304 (2015).
- [30] V. Makhalov, K. Martiyanov, and A. Turlapov, *Phys. Rev. Lett.* **112**, 045301 (2014).
- [31] B. Fröhlich, M. Feld, E. Vogt, M. Koschorreck, W. Zwerger, and M. Köhl, *Phys. Rev. Lett.* **106**, 105301 (2011).
- [32] W. Ong, C.-Y. Cheng, I. Arakelyan, and J. E. Thomas, *Phys. Rev. Lett.* **114**, 110403 (2015).
- [33] M. G. Ries, A. N. Wenz, G. Zurn, L. Bayha, I. Boettcher, D. Kedar, P. A. Murthy, M. Neidig, T. Lompe, and S. Jochim, *Phys. Rev. Lett.* **114**, 230401 (2015).
- [34] A. T. Sommer, L. W. Cheuk, M. J. H. Ku, W. S. Bakr, and M. W. Zwierlein, *Phys. Rev. Lett.* **108**, 045302 (2012).
- [35] V. L. Berezinskii, *Sov. Phys. JETP* **32**, 493 (1971); **34**, 610 (1972); J. M. Kosterlitz and D. Thouless, *J. Phys. C* **5**, L124 (1972); **6**, 1181 (1973).
- [36] D. R. Nelson and B. I. Halperin, *Phys. Rev. B* **19**, 2457 (1979).
- [37] A. P. Young, *Phys. Rev. B* **19**, 1855 (1979).
- [38] D. S. Petrov, M. A. Baranov, and G. V. Shlyapnikov, *Phys. Rev. A* **67**, 031601(R) (2003).
- [39] W. Zhang, G.-D. Lin, and L.-M. Duan, *Phys. Rev. A* **78**, 043617 (2008).
- [40] M. Iskin and C. A. R. Sa de Melo, *Phys. Rev. Lett.* **103**, 165301 (2009).
- [41] J. Tempere, S. N. Klimin, and J. T. Devreese, *Phys. Rev. A* **79**, 053637 (2009).
- [42] S. N. Klimin, J. Tempere, and J. T. Devreese, *New J. Phys.* **14**, 103044 (2012).
- [43] L. Salasnich, P. A. Marchetti, and F. Toigo, *Phys. Rev. A* **88**, 053612 (2013).
- [44] P. A. Murthy, I. Boettcher, L. Bayha, M. Holzmann, D. Kedar, M. Neidig, M. G. Ries, A. N. Wenz, G. Zurn, and S. Jochim, *Phys. Rev. Lett.* **115**, 010401 (2015).
- [45] L. He and X.-G. Huang, *Phys. Rev. Lett.* **108**, 145302 (2012).
- [46] J. P. A. Devreese, J. Tempere, and C. A. R. Sá de Melo, *Phys. Rev. Lett.* **113**, 165304 (2014).
- [47] J. P. A. Devreese, J. Tempere, and C. A. R. Sa de Melo, *Phys. Rev. A* **92**, 043618 (2015).
- [48] Y. Xu and C. Zhang, *Phys. Rev. Lett.* **114**, 110401 (2015).
- [49] Y. Cao, X.-J. Liu, L. He, G.-L. Long, and H. Hu, *Phys. Rev. A* **91**, 023609 (2015).
- [50] E. Abrahams and T. Tsuneto, *Phys. Rev.* **152**, 416 (1966).
- [51] A. J. Leggett, *Quantum Liquid* (Oxford University Press, Oxford, 2006).
- [52] S. Doniach and B. A. Huberman, *Phys. Rev. Lett.* **42**, 1169 (1979).
- [53] S. S. Botelho and C. A. R. Sá de Melo, *Phys. Rev. Lett.* **96**, 040404 (2006).
- [54] H. Hu, X.-J. Liu, and P. D. Drummond, *Europhys. Lett.* **74**, 574 (2006).
- [55] R. B. Diener, R. Sensarma, and M. Randeria, *Phys. Rev. A* **77**, 023626 (2008).
- [56] L. He, H. Lu, G. Cao, H. Hu, and X. J. Liu, *Phys. Rev. A* **92**, 023620 (2015).
- [57] G. Bighin and L. Salasnich, *Phys. Rev. B* **93**, 014519 (2016).
- [58] B. C. Mulkerin, L. He, P. Dyke, C. J. Vale, X.-J. Liu, and H. Hu, *Phys. Rev. A* **96**, 053608 (2017).
- [59] G. Sarma, *J. Phys. Chem. Solid* **24**, 1029 (1963).
- [60] A. I. Larkin and Yu. N. Ovchinnikov, *Sov. Phys. JETP* **20**, 762 (1965).
- [61] P. Fulde and R. A. Ferrell, *Phys. Rev.* **135**, A550 (1964).
- [62] S. Takada and T. Izuyama, *Prog. Theor. Phys.* **41**, 635 (1969).
- [63] M. W. Zwierlein, A. Schirotzek, C. H. Schunck, and W. Ketterle, *Science* **311**, 492 (2006).
- [64] G. B. Partridge, W. Li, R. I. Kamar, Y.-an Liao, R. G. Hulet, *Science* **311**, 503 (2006).
- [65] D. E. Sheehy and L. Radzihovsky, *Phys. Rev. Lett.* **96**, 060401 (2006).
- [66] H. Zhai, *Rep. Prog. Phys.* **78**, 026001 (2015).